# Supplementary Information for

## *kinITC*: a new method for obtaining joint thermodynamic and *kinetic* data by Isothermal Titration Calorimetry

Dominique Burnouf[1], Eric Ennifar[1], Sondes Guedich, Barbara Puffer[ǂ], Guillaume Hoffmann, Guillaume Bec, François Disdier, Mireille Baltzinger[†] & Philippe Dumas*

This document presents first the theoretical and practical aspects of the new method, then information on the experimental systems used and, finally, illustrations on several experimental results.

## *1-Web site for the illustration of several points*

We have developed a web site for illustrating several points about the baseline correction, the instrument response time, the simulation of data and the visualization of real experimental data.

http://www-ibmc.u-strasbg.fr:8080/webMathematica/kinITCdemo/

## *2-Influence of the instrument response time*

The major effect influencing the shape of the titration curves results from the response time of the calorimeter. This is defined by the characteristic time of the exponential decrease of the signal after an 'instantaneous' heat impulse delivered in the cell measurement. We determined it with short-time electric impulses (used normally for calibrating the instrument), as well as with heat from the dilution of quickly injected methanol. The results showed slight variations but they nevertheless gave consistent results: (3.4 ± 0.4) s from the electric impulses, and (3.2 ± 0.12) s and (3.7 ± 0.7) s from methanol injections giving rise, respectively, to small and large amplitude responses. This is a remarkably short response time in comparison of that reported [1] for an old-generation instrument (15 s) with a measurement cell volume (5 ml) much larger than the 0.2 ml for our new-generation instrument. We currently used $\tau_{ITC} = 3.5$ s in our simulations.

The influence of this response time was discussed in the frame of Differential Scanning Calorimetry [2]. More recently, it was taken into account for ITC data [3]. It is accounted for by expressing the measured power $P_m(t)$ as the convolution of the effectively delivered signal $P_s(t)$ with an exponential kernel $R(t) = 1/\tau_{ITC} \exp(-t/\tau_{ITC})$. This is expressed as:

$$P_m(t) = \frac{1}{\tau_{ITC}} \int_0^t e^{-(t-\theta)/\tau_{ITC}} P_s(\theta) d\theta = \frac{1}{\tau_{ITC}} e^{-t/\tau_{ITC}} \int_0^t e^{\theta/\tau_{ITC}} P_s(\theta) d\theta \qquad (1)$$

To obtain $P_m(t)$ from $P_s(t)$ one can then either invoke a Laplace transform [2], or simply perform two successive derivations of $P_m(t)$ from the previous expression, which yields:

$$P_m'(t) + \tau_{ITC} P_m''(t) = P_s'(t)$$

This is readily integrated as (the integration constant has to be zero):

$$P_m(t) + \tau_{ITC} P_m'(t) = P_s(t) \qquad (2)$$

Therefore, if a kinetic model allows calculating the instantaneous heat power $P_s(t)$ evolved in the measurement cell, the effectively measured heat power $P_m(t)$ can be obtained by (numerical) integration of equation (2). This is illustrated with Fig. S1A.

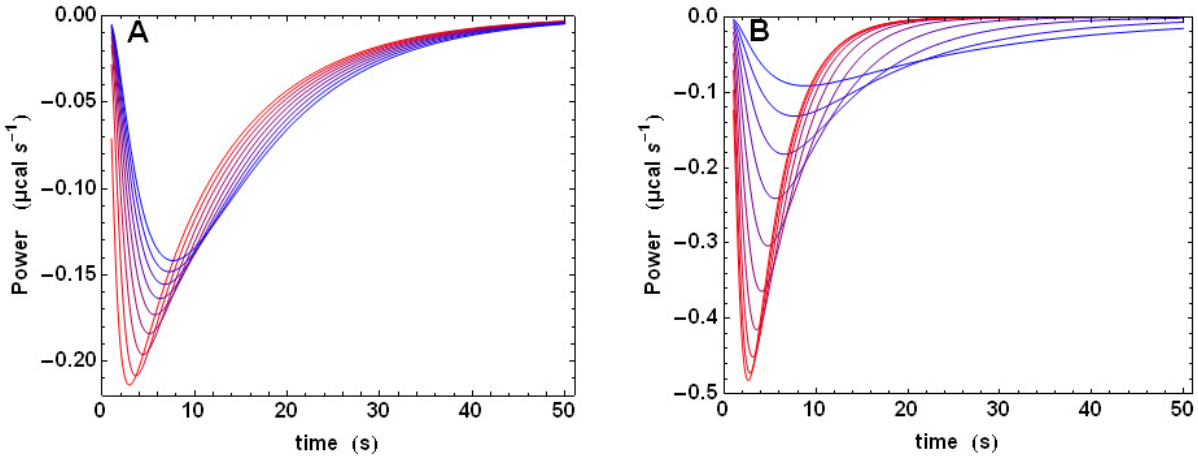


**Fig. S1 (A) Influence of the instrument response time**. Simulated power curves $P_m(t)$ for the first injection of a titration with the instrument response time varying from 0 s (red) to 4.5 s (blue) by steps of 0.5 s. The values used for the simulations were:
$k_{on} = 2\times10^4$ M$^{-1}$s$^{-1}$, $K_d = 0.1\,\mu$M, $\Delta H = -20$ kcal mol$^{-1}$, $[A] = 5$ µM, $[B] = 60$ µM, and injected volume = 2.3 µl, injection time = 0.5 s, integration time = 1 s, mixing time = 0.8 s.
Note that the simulation yields a continuous curve, whereas the instrument yields a discrete sampling of it at intervals equal to the integration time.
**(B) Influence of the association constant $k_{on}$**. Same as in A, but with a constant response time of 3.5 s and $k_{on}$ values decreasing from $10^6$ $M^{-1}$s$^{-1}$ (red) to $10^4$ $M^{-1}$s$^{-1}$ (blue) in equal logarithmic steps.

The correlation with the effect of the variation of the kinetic parameter $k_{on}$ at constant response time is shown with Fig. S1B. From this comparison, one may infer that the relative

error on the determination of $k_{on}$ due to the error on $\tau_{ITC}$ $\delta k_{on}/k_{on} \sim \delta\tau_{ITC}/\tau_{ITC}$ is less than 0.3/3.5 ~ 8 %. However, this is valid for not too high $k_{on}$ values, because beyond some threshold, all $k_{on}$ values yield the same limiting power curve defined by $\tau_{ITC}$ (see the two last red curves on Fig. S1B corresponding to $0.6\times10^6$ and $10^6$ $M^{-1}s^{-1}$ ). This is examined in more details in the following (§ 5).

## *3-Influence of the finite injection and mixing times*

Independently of the instrument response time one has to take into account that neither the injection nor the mixing of compound B is instantaneous. This is illustrated with Fig. S2.

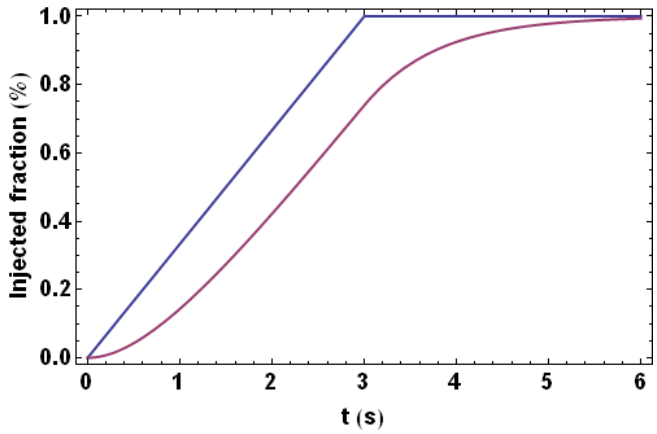


**Fig. S2. Influence of the mixing time during a finite-time injection.** The upper broken line corresponds to an injection during a finite time (here 3 s). It is unattainable in practice, since this requires instantaneous mixing of the injected species. The lower smooth curve corresponds to a realistic simulation by considering a finite mixing time $\tau_{mix}$. This is modelled by a convolution of the ideal upper line with an exponential kernel $1/\tau_{mix}\exp(-t/\tau_{mix})$. Here $\tau_{mix}$ = 0.8 s. If it is doubtless that $\tau_{mix} \neq 0$, it is not yet very clear what is its exact link with the speed of rotation of the mixer. We have used in this work $\tau_{mix}$ = 0.8 rpm/1000, where rpm is the speed of rotation in revolutions per minute. This is likely to be improved in the future.

## *4-Equilibration-time variation along a titration experiment and its practical importance*

Here, we consider a situation corresponding to the simple scheme $A + B \underset{k_{off}}{\overset{k_{on}}{\rightleftarrows}} C$, with $[A]_0 = [A] + [C]$ and $[B]_0 = [B] + [C]$ being the total concentrations of the compounds A and B. Its evolution is described by the differential equation $dC/dt = k_{on}[A]_0 A\, B - k_{off} C$ with $A = [A]/[A]_0$, $B = [B]/[A]_0$ and $C = [C]/[A]_0$ (see main text). Its general solution for any injection is obtained as:

$$C(t) = \frac{C_1 - K C_2 e^{t/\tau}}{1 - K e^{t/\tau}} \tag{3}$$

where $\tau^{-1} = k_{on}[A]_0 (C_1 - C_2)$, $C_1$ and $C_2$ $(C_1 > C_2)$ being the roots of the equation $[A]_0 (1 - C)(B_0 - C) - K_d C = 0$, and $K$ is the integration constant defining the initial value $C(0)$ of the reduced concentration (for this theoretical study the time always starts at 0 for all injections). The heat power evolved in the measurement cell is $P_s(t) = V_{cell}\, \Delta H [A]_0\, dC/dt$ (see main text). It is easily shown that, for any value of $K$, the logarithmic derivative of $dC/dt$, and thus also of $P_s(t)$, continuously evolves from $-\tau_0^{-1}$ for $t = 0$ to $-\tau^{-1}$ for $t \to \infty$ (it would be exactly constant for an exponential function). It is also shown that the ratio $\tau/\tau_0 \approx 1/2\left([A]_0 + [B]_0\right)/\left([A]_0 [B]_0\right)^{1/2} > 1$ since an arithmetic mean is always greater than a geometric mean. Therefore, $\tau$ is an upper limit of the characteristic time of the exponential-like function $P_s(t)$.

We now examine the behaviour of $\tau$ from injection to injection. Taking in consideration the terms $C_1$ and $C_2$, it is obtained:

$$\tau = \frac{1/c}{k_{off}\left[\left(1/c + B_0 + 1\right)^2 - 4B_0\right]^{1/2}} \tag{4}$$

where $B_0 = [B]_0/[A]_0$ is the stoichiometric ratio and $c = [A]_0/K_d$ the Wieseman parameter. This expression is valid for any injection during a titration experiment, which means that the total concentrations $[A]_0$ and $[B]_0$ vary from injection to injection. However, when the stoichiometric ratio $B_0$ increases steadily during an experiment, the concentration $[A]_0$ only

decreases slightly due to the dilution. Therefore, with the approximation $[A]_0 \sim$ constant, equation (4) implies that $\tau$ increases from a minimum value $\tau_1 \approx \boldsymbol{k}_{\boldsymbol{off}}^{-1}(1+\boldsymbol{c})^{-1}$ at the first injection, to a maximum value $\tau_{max} \approx 1/2\, \boldsymbol{k}_{\boldsymbol{off}}^{-1}\, \boldsymbol{c}^{-1/2}$ for a stoichiometric ratio $\boldsymbol{B}_0 = 1 - 1/\boldsymbol{c}$, which is very close to mid-titration in general. If one considers that $\boldsymbol{C}(\boldsymbol{t})$ does not evolve any more for $\boldsymbol{t} > 4\,\tau$, one obtains the following useful results about the equilibration times $\theta_1$ for the first injection and $\theta_{max}$ at mid-titration:

$$\theta_{max} / \theta_1 = 1/2\left(\boldsymbol{K}_{\boldsymbol{d}} + [A]_0\right) / \left(\boldsymbol{K}_{\boldsymbol{d}}\,[A]_0\right)^{1/2} \sim 1/2\,\boldsymbol{c}^{1/2} \qquad (5a)$$

$$\theta_{max} \sim 2\,\boldsymbol{k}_{\boldsymbol{off}}^{-1}\,\boldsymbol{c}^{-1/2} = 2\left(\boldsymbol{k}_{\boldsymbol{off}}\,\boldsymbol{k}_{\boldsymbol{on}}\,[A]_0\right)^{-1/2} \qquad (5b)$$

Equation (5a) implies that the equilibration time may vary considerably from the first injection to mid-titration, since $\boldsymbol{c} \sim 100$ is not unusual. Such a variation can be seen on a great number of ITC curves reported in publications. It is shown with calculated data (FigS3). An interesting consequence is that these results may allow deriving 'at a glance' the values of $\boldsymbol{K}_{\boldsymbol{d}}$, $\boldsymbol{k}_{\boldsymbol{on}}$ and $\boldsymbol{k}_{\boldsymbol{off}}$. This is illustrated with the right panel of Fig. S3A, which shows superimposed the first injection and the mid-titration injection (purple), as well as two arrows corresponding to $\theta_1$ and $\theta_{max}$. These two arrows were quickly positioned 'by eye'. A simple correction to these values was made by subtracting the sum (injection time $+\tau_{\boldsymbol{ITC}}$) = 4 s, which yielded $\theta_1$ = 49 s and $\theta_{max}$ = 230 s. Together with equation (5a), these values yielded $\boldsymbol{c} \sim 89$ (exact value used in the calculation: 110), which in turn yielded (with $[A]_0 = 11$ µM) $\boldsymbol{K}_{\boldsymbol{d}} \sim$ 0.12 µM (exact value 0.1 µM). Finally, equation (5b) led to $\boldsymbol{k}_{\boldsymbol{off}} \sim 8.8\ 10^{-4}\ s^{-1}$ (exact value $10^{-3}\ s^{-1}$), which implies $\boldsymbol{k}_{\boldsymbol{on}} \sim 7110\ M^{-1}\ s^{-1}$ (exact value $10^4\ M^{-1}\ s^{-1}$). Considering the simplicity of the method, these results are worth of interest. Obviously, the quality of the method is the best for slow kinetics that are less affected by $\tau_{\boldsymbol{ITC}}$. In addition, it should be strongly emphasized that this simplified treatment is **only valid for mechanisms that are correctly represented by simple on/off kinetics**. Therefore, the full treatment remains necessary for assessing the validity of such quickly-obtained results.

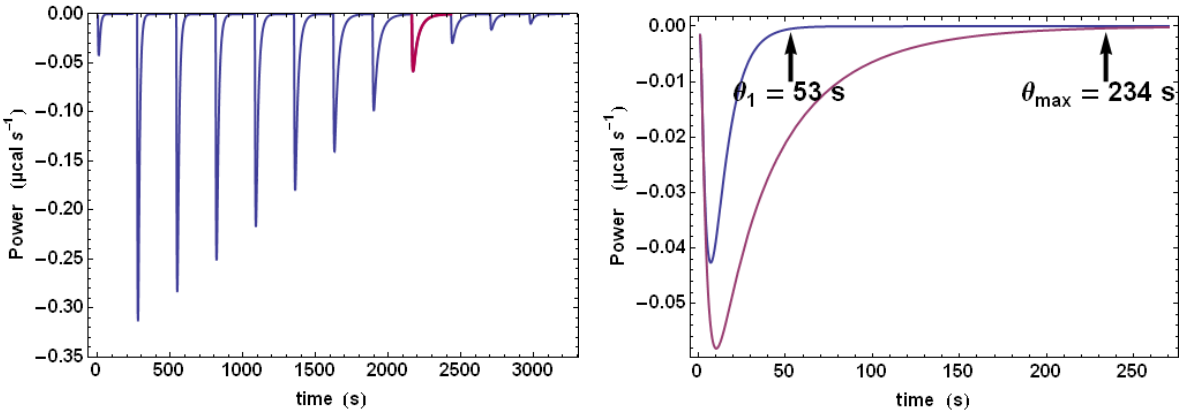


**Fig. S3A Evolution of the equilibration time and its use for deriving $K_d$, $k_{on}$ and $k_{off}$.** The left-panel titration curve was obtained with the values $\tau_{ITC}$ = 3.5 s, $\tau_{mix}$ = 0.8 s, $[A]_0$ = 11 µM, $[B]_0$ = 120 µM, $k_{on}$ = $10^4$ s$^{-1}$, $K_d$ = 0.1 µM. The injected volume was 0.3 µl for the first injection and 2.3 µl otherwise. The purple curves on the two panels correspond to mid-titration, the blue curve on the right panel corresponds to the first injection. See text for explanations.

The method was applied with data from RT/Nevirapine (Fig. S3B). Given the very low signal-to-noise ratio with the two injections to be used, the localization of $\theta_1$ and $\theta_{max}$ was not as obvious as with the calculated data of Fig. S3A. With the values obtained for $\theta_1$ and $\theta_{max}$, the following values were calculated (in the order 25, 30 and 35 °C):

$K_d$ : 3.4, 4.0, 1.8 µM (values from curve fitting: 2.2, 3.5, 5.4 µM)

$k_{on}$ : 1139, 1728, 4364 M$^{-1}$ s$^{-1}$ (values from curve fitting: 1200, 1900, 3000 M$^{-1}$ s$^{-1}$ )

$k_{off}$ : 0.0039, 0.0070, 0.0078 s$^{-1}$ (values from curve fitting: 0.0025, 0.007, 0.015 s$^{-1}$ )

The method was thus rather efficient despite a very unfavourable signal-to-noise ratio.

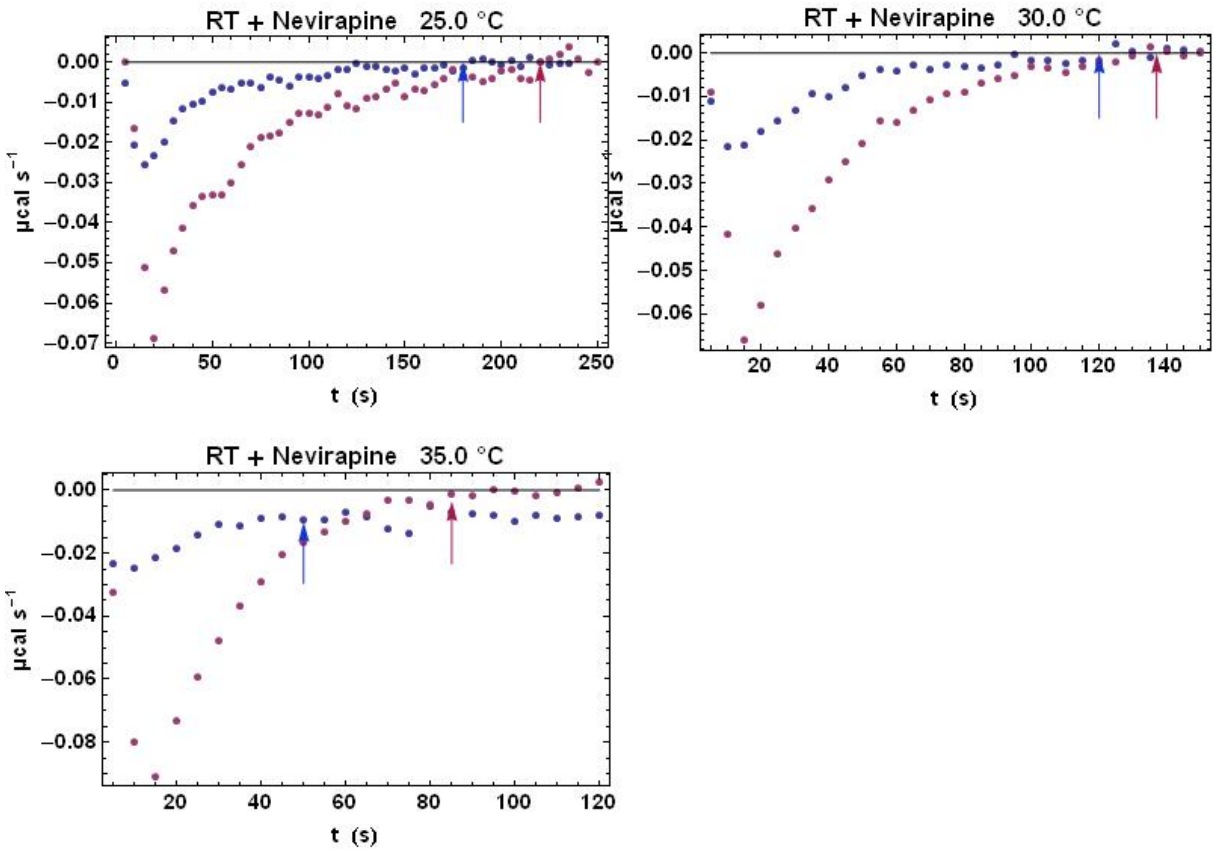


**Fig. S3B Use of $\theta_1$ and $\theta_{max}$ for deriving $K_d$, $k_{on}$ and $k_{off}$ with RT+Nevirapine.** The method is the same as in Fig. S3A. For the three temperatures the Nevirapine (compound A) was at an initial concentration $[A]_0$ = 20 µM. The values of the Wieseman parameter $\boldsymbol{c} = [A]_0/K_d$ determined from $\theta_{max}/\theta_1 \sim 1/2\,\boldsymbol{c}^{1/2}$ were 5.8, 4.9, 11.2 for 25, 30, 35 °C, respectively.

## *5-Range of application of kinITC*

Another consequence of interest is about the range of application of *kinITC*. As a crude rule of thumb, one may consider that an exponential-like power signal defined by a characteristic time $\tau$ begins being discernable from the instrument response function if $\tau > \tau_{ITC}/10$. Therefore, from $\tau_{max} \approx \left(2\boldsymbol{k}_{off}\right)^{-1} \boldsymbol{c}^{-1/2}$, the following inequality involving the dimensionless quantities $\Theta_{on} = \left(\boldsymbol{k}_{on}\left[A\right]_0 \tau_{ITC}\right)$ and $\Theta_{off} = \left(\boldsymbol{k}_{off}\tau_{ITC}\right)$, should hold for having a chance of discerning a kinetic signal, and not merely the instrument response function:

$$\Theta = \left(\Theta_{on}\,\Theta_{off}\right)^{1/2} < 5 \qquad (6a)$$

Other equivalent forms of this are:

$$\Theta = \boldsymbol{k}_{off}\,\tau_{ITC}\,\boldsymbol{c}^{1/2} = \left(\boldsymbol{k}_{on}\,\boldsymbol{k}_{off}\left[A\right]_0\right)^{1/2}\tau_{ITC} < 5 \qquad (6b)$$

The upper value of 5 is considerably optimistic and, in practice, significantly lower values should be considered to take into account the quality of the experimental data. It is probably more realistic to consider an upper value of 2 for good-quality data. This will be defined firmly only when more different cases are known.

## 6-Temperature variation of dissociation 'constants' $K_d$

The thermodynamically rigorous Van t'Hoff equation $\partial\left(\boldsymbol{Ln}\,\boldsymbol{K}_d\right)/\partial\boldsymbol{T} = -\Delta\boldsymbol{H}/\left(\boldsymbol{R}\,\boldsymbol{T}^2\right)$ yields $\boldsymbol{K}_d\left(\boldsymbol{T}\right)$ explicitly if $\Delta\boldsymbol{H}(\boldsymbol{T})$ is known. Usually, $\Delta\boldsymbol{C}_p = \partial\boldsymbol{H}/\partial\boldsymbol{T}$ may be considered constant to a good approximation. However, as we have seen with TPP riboswitch folding, there are situations where $\Delta\boldsymbol{C}_p$ itself is temperature-dependent ($\partial\Delta\boldsymbol{C}_p/\partial\boldsymbol{T} = \alpha \neq 0$). In the most general situation, therefore, we consider the following set of equations, the last one being the integrated form of the Van t'Hoff equation:

$$\Delta\boldsymbol{C}_p = \Delta\boldsymbol{C}_p^0 + \alpha\left(\boldsymbol{T} - \boldsymbol{T}^0\right) \tag{7a}$$

$$\Delta\boldsymbol{H} = \Delta\boldsymbol{H}^0 + \Delta\boldsymbol{C}_p^0\left(\boldsymbol{T} - \boldsymbol{T}^0\right) + \alpha/2\left(\boldsymbol{T} - \boldsymbol{T}^0\right)^2 \tag{7b}$$

$$\boldsymbol{K}_d\left(\boldsymbol{T}\right) = \boldsymbol{K}_d^0\left(\boldsymbol{T}^0/\boldsymbol{T}\right)^{\beta/\boldsymbol{R}} \exp\left[(1-\boldsymbol{T}^0/\boldsymbol{T})\left(\gamma - \alpha(\boldsymbol{T}+\boldsymbol{T}^0)/2\right)/\boldsymbol{R}\right] \tag{7b}$$

with $\beta = \Delta\boldsymbol{C}_p^0 - \alpha\boldsymbol{T}^0$, $\gamma = \Delta\boldsymbol{C}_p^0 - \Delta\boldsymbol{H}^0/\boldsymbol{T}^0$ and the superscript 0 referring to values at an arbitrary reference temperature $\boldsymbol{T}^0$.

## 7-Baseline correction (see web site)

Accurate baseline correction is particularly important for *kinITC* since we need obtaining as accurately as possible the shape of each injection curve, and not only their integrated values. This is a task that is still under development in view of obtaining more automatic procedures, particularly for removing aberrant discontinuities. Here, we have used semi-automated methods based upon the determination of a smooth interpolation curve between a set of few points per injection, each point being obtained by averaging several contiguous points of the raw curve. In order to define the baseline these contiguous points are selected close to the end of each injection. The results of baseline correction for RT+Nevirapine are shown with Fig. S4.

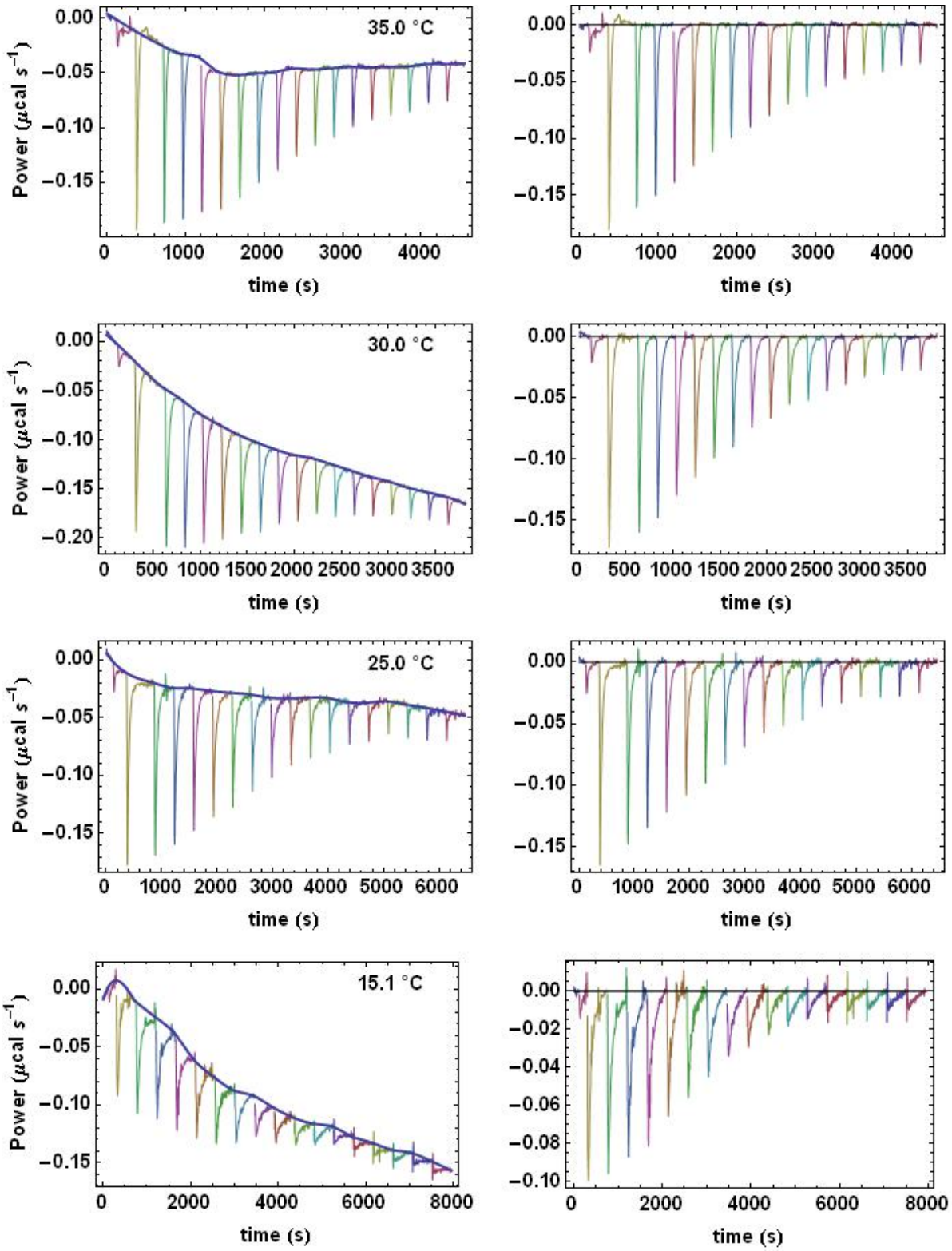


**Fig. S4. Baseline correction of experimental curves.** Left column: raw experimental curves for RT+Nevirapine along with their baseline. Right column: corrected experimental curves. The experiment at 15.1 °C led to poor data and the time left for each injection was insufficient, which prevented from obtaining correct baselines. These data were not used.

## *8-Fitting of the titration curves for retrieving kinetic information*

The overall flow of the method in use to recover kinetic information is the following.

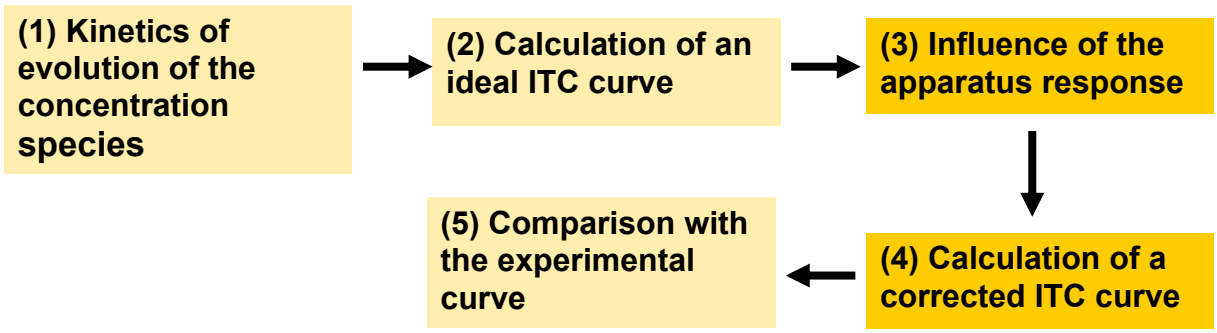


**Step (1)** corresponds to considering a kinetic model to account for the evolution of all concentrations after each injection of compound B. In the most simple situation, one considers the association/dissociation process $A + B \underset{k_{off}}{\overset{k_{on}}{\rightleftarrows}} C$ .

**Step (2)** corresponds to integrating the differential equation (equation 5 in the main text), or the set of differential equations (equations 9a,b in the main text), describing the evolution of concentrations. At this step, one already takes into account both the finite injection time and the finite mixing times (Fig. S2). Therefore, even in the most simple case leading to an analytical solution of the differential equation (equation 6 in the main text and equation 3 in this document), one has to perform a numerical integration to take into account the progressive injection and mixing of compound B. This procedure yields a function $P_s(t)$ (equation 7 in the main text).

**Step (3)** allows taking into account the instrument response time to obtain $P_m(t)$ by numerically integrating equation 2 in this document.

**Step (4)** allows calculating a theoretical ITC curve fully comparable to an experimental one. For that, one has to take into account that each experimental curve corresponds to a succession of measurements at regular interval, each measurement being an average of the heat power evolved between two successive measurements separated by the 'integration time' $\delta$t (indicated in Table 1). This explains that the experimental curves never start at $t = 0$ but at $t = \delta$t. In fact, because $\delta$t is small, this amounts to applying a small correction to $P_m(t)$.

**Step (5)** is for comparing all theoretical power curves to their experimental counterparts (after baseline correction). This is done with a non-linear least-squares procedure, which allows adjusting the free parameters. A starting set of these is obtained by trial and errors. In this work we have used the procedure 'FindMinimum' in *Mathematica.*

## *9-Information on the macromolecules used*

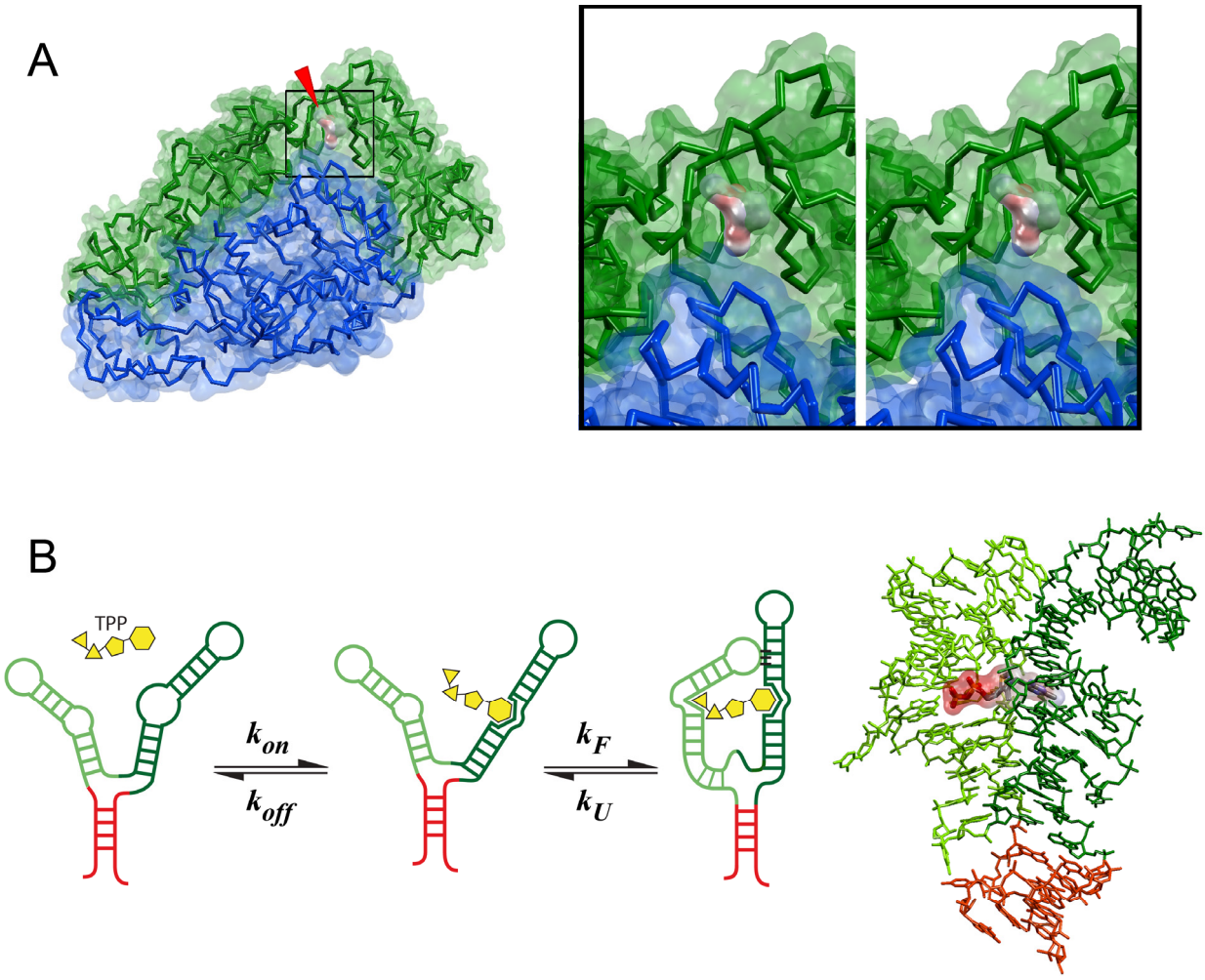


**Fig. S5. (A) Structure of HIV-1 Reverse Transcriptase and of Nevirapine binding site.** The zoom on the right-hand side (crossed-eye stereo) highlights the hydrophobic Nevirapine buried inside the protein (PDBID: 1VRT).

**(B) Scheme of the interaction between *E. coli* TPP riboswitch and its ligand.** This illustrates the mechanism mentioned in equations 2a,b. Note that this is only schematic and that it does not imply that all secondary structures are formed before complete folding/closing of the structure. The rightmost figure shows the 3D crystal structure of the related TPP riboswitch from *A. thaliana* (PDBID: 2CKY).

## *10-Results from the fitting procedure for RT+Nevirapine (see web site)*

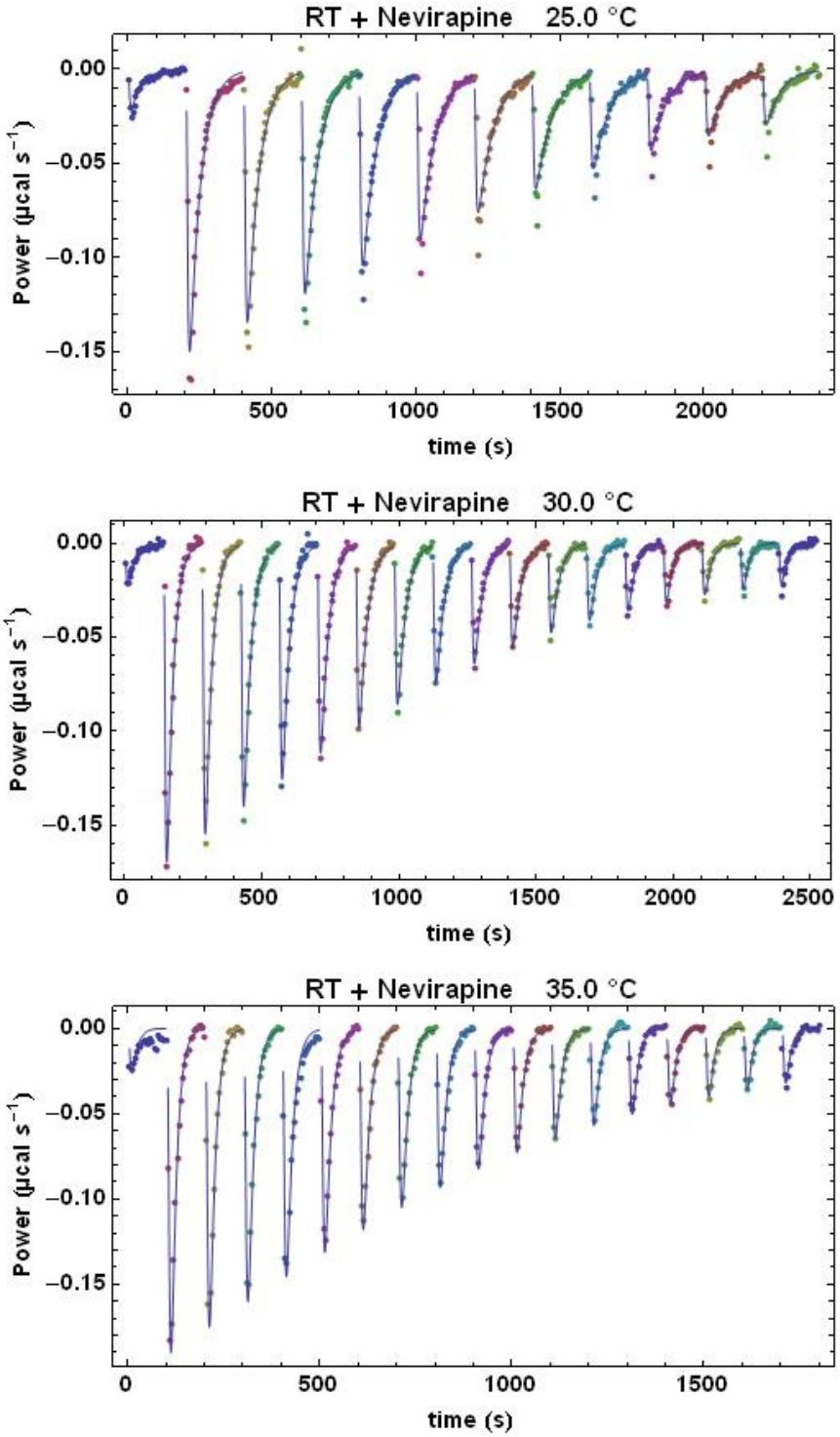


**Fig. S6. Kinetic fit of all baseline-corrected titration curves for RT+Nevirapine.**
Only the injections and only their part used in the fitting procedure for each experiment are shown. Less injections were used for fitting the experiment at 25 °C due to a more important contribution at that temperature of a small heat signal of unknown origin.

## *11-Global thermodynamic treatment of the TPP riboswitch titration curves*

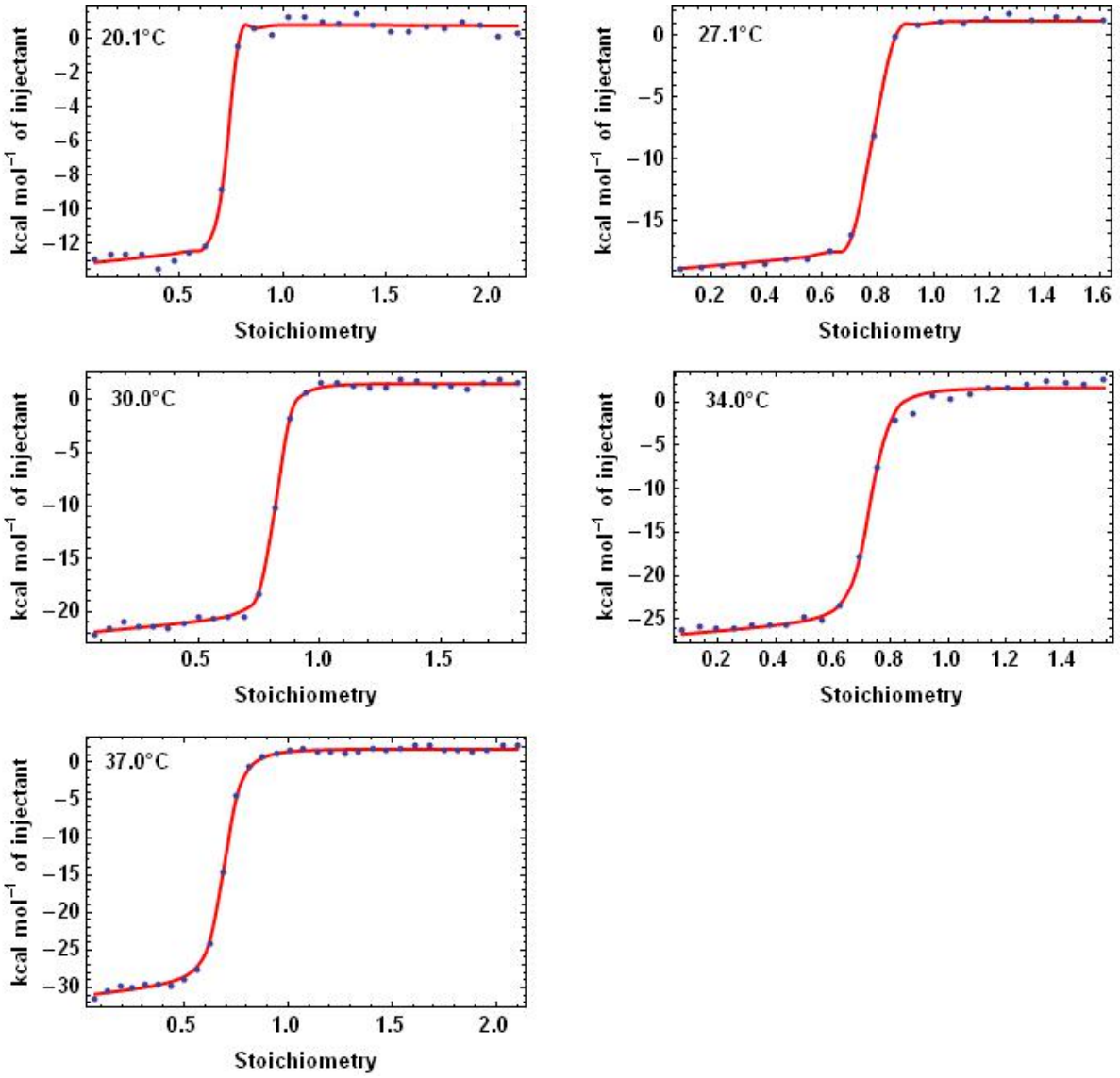


**Fig. S7. ITC titration curves for the *E. coli* TPP riboswitch**
The dots correspond to the integrated heats for each injection and the red curves correspond to the fit obtained by 'global thermodynamic treatment' of all experiments. It was necessary to take into account an 'active fraction' of the RNA since the inflexion point in each titration curve was at a stoichiometry significantly lower than 1, which is in no way exceptional. The initial global thermodynamic treatment led from 20 °C to 37 °C to the following RNA active fractions: 0.69, 0.74, 0.79, 0.70, 0.66. After fitting all titration curves by *kinITC* it was obtained: 0.675, 0.745, 0.776, 0.686, 0.639.

## *12-Results from the fitting procedure for the TPP riboswitch*

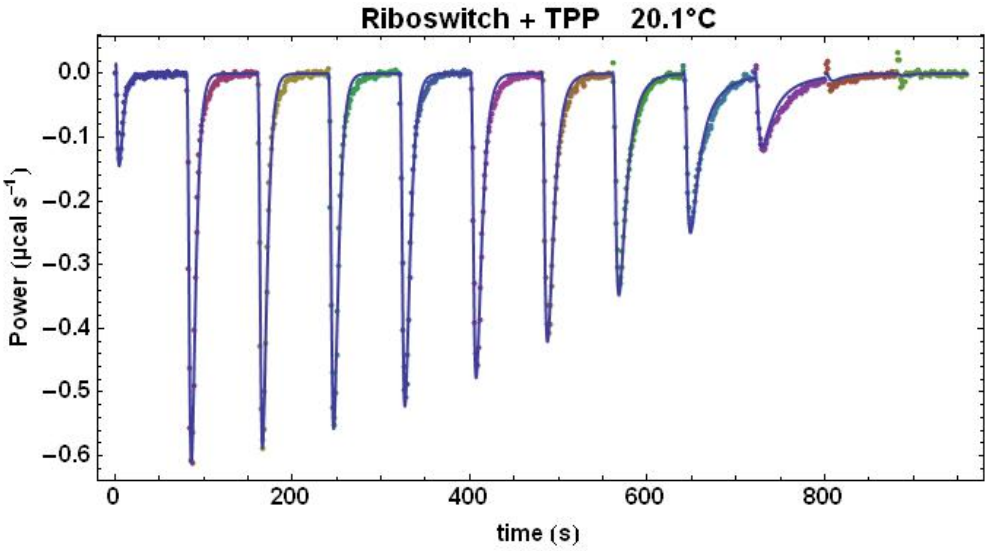


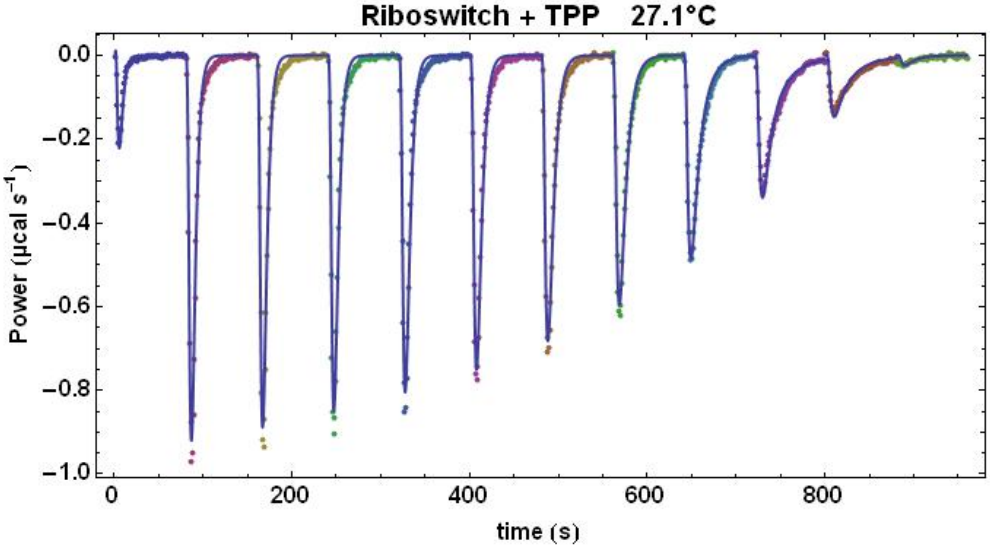


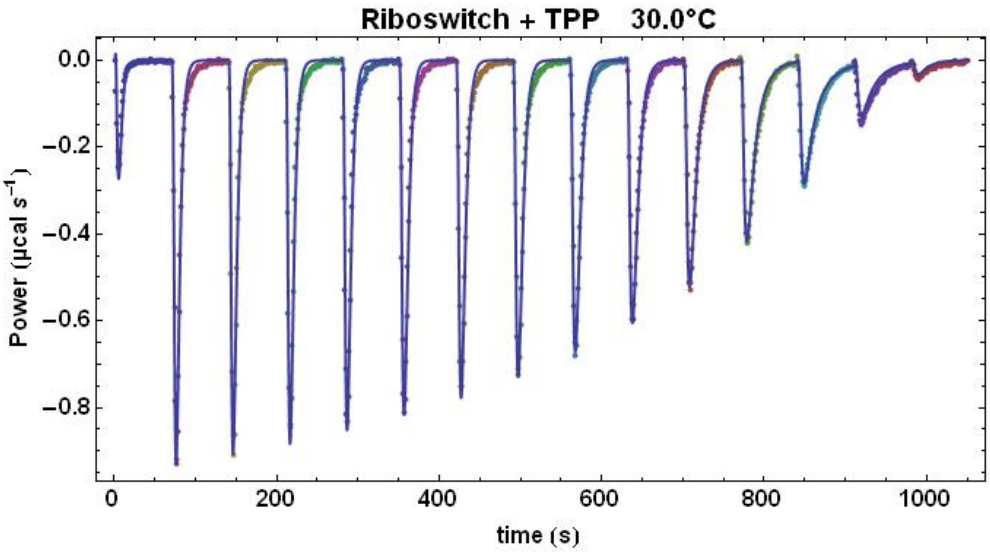

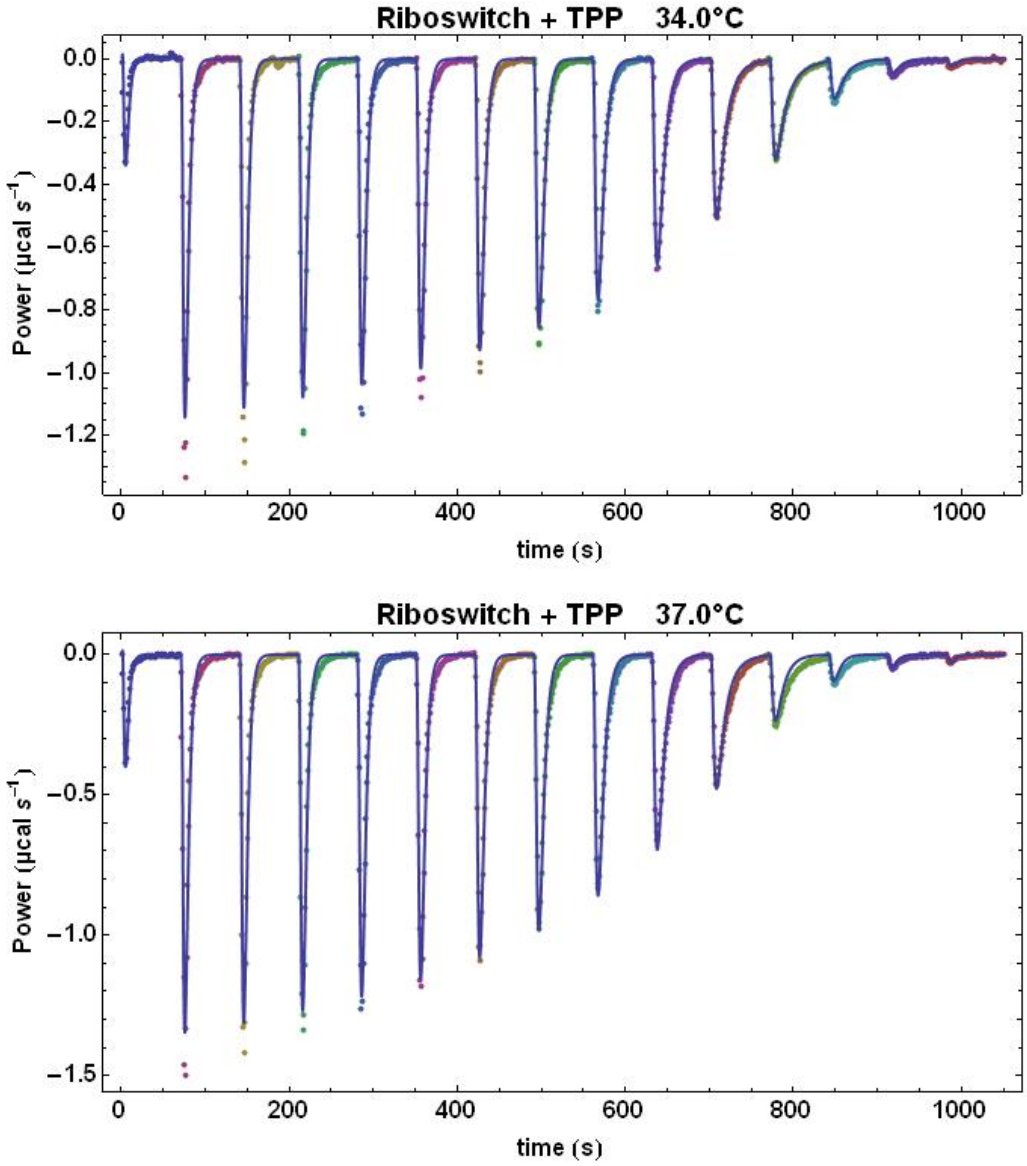


**Fig. S8. Kinetic fit of all baseline-corrected titration curves for TPP+Riboswitch.**
Only the injections used in the fitting procedure for each experiment are shown. The variation of amplitude and width of each injection curve is well recovered, even for the first one which is often disregarded since it is made in prevision of a possible backlash of the injection pump. One may nevertheless notice the slight, but systematic, lack of fit occurring in a time-range centered around 30 s after the beginning of each injection. This is striking because the experimental data were of very good quality. We have no explanation for this.

## *13-Hydroxyl-radical footprint experiment*

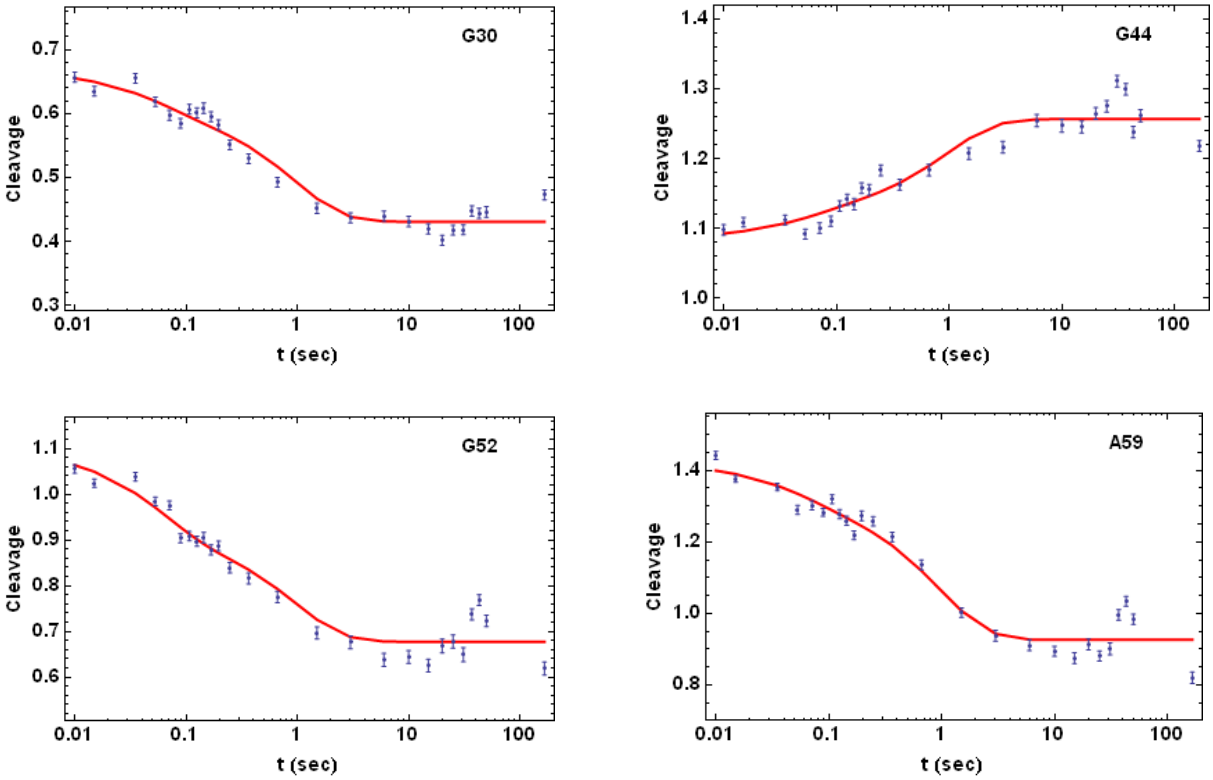


**Fig. S9. Representative sample of kinetic curves of *E. coli thiC* TPP riboswitch folding obtained by $OH^{\bullet}$ footprinting (to be published).** The experimental points and their error bars were obtained by electrophoresis gel quantification. The cleavage is expressed in arbitrary units. The red curves are theoretical curves obtained with the same kinetic model as the one used for the *kinITC* experiments. This model thus explains equally well these two totally independent experiments. Note that we tested an alternative kinetic model with these chemical footprinting data. The alternative hypothesis was to consider that the binding of the TPP did not trigger RNA folding, but instead occurred only after RNA folding. This model was unable to explain the short-time variation of the cleavage.
As shown by this representative sample, there is a strong tendency of a decrease of the cleavage, which fits with the increased protection against the hydroxyl radicals during the folding. It also may be noticed that the evolution of this folding-dependent cleavage reaches a plateau after a few seconds, which readily indicates that the rate of folding $k_F$ lies around 1 $s^{-1}$.

## *14-Surface Plasmon Resonance experiments*

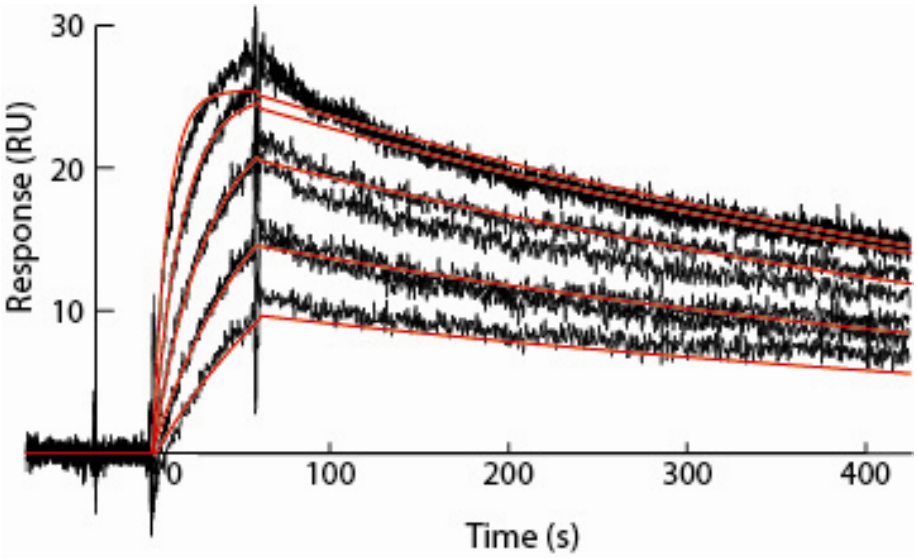


**Fig. S10. SPR experiment for RT/Nevirapine**. Experimental data collected for each nevirapine solution, from bottom to top at 3.5, 6.3, 12.5, 25 and 50 µM. The experiments were replicated twice at each concentration (except for 3.5 µM). Theoretical curves (red) were obtained with a simple bimolecular reaction model and parameters $k_{on}$ = 2,4×10$^{3}$ M$^{-1}$ s$^{-1}$, $k_{off}$ = 1.5×10$^{-3}$ s$^{-1}$, $R_{max}$ = 25 RU.

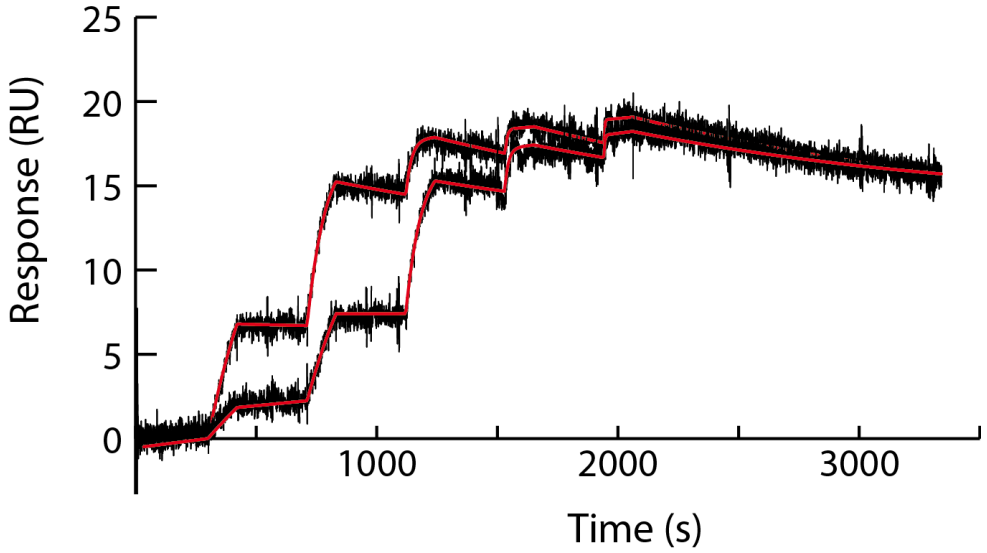


**Fig. S11. SPR experiment for the TPP riboswitch**.
The two sensorgrams were obtained in independent experiments. A 3-fold (upper curve) or 4-fold (lower curve) increase in TPP concentration was used at each successive injection. The concentrations were 0.037, 0.11, 0.33, 1, 3µM (upper cruve) and 0.007, 0.03, 0.125, 0.5, 2µM (lower curve). Theoretical curves (red), assuming a simple 1:1 association model, were obtained with the following kinetic parameters:

$k_{on}$ = 1.33 ×10$^{5}$ M$^{-1}$.s$^{-1}$, $k_{off}$ = 2.91×10$^{-4}$ s$^{-1}$ and $R_{max}$ = 16.8 RU (upper curve)
$k_{on}$ = 1.33 ×10$^{5}$ M$^{-1}$.s$^{-1}$, $k_{off}$ = 3.1×10$^{-4}$ s$^{-1}$ and $R_{max}$ = 15 RU (lower curve)

## *15-Summary of quantitative results*

Here are collected the final results obtained with RT/Nevirapine and the TPP riboswitch after kinetic fit of the injection curves. All values for quantities with a superscript 0 correspond to the reference temperature $T^0$ = 30 °C.

### Results for RT + Nevirapine

All values are given twice. The first value corresponds to the results after treatment of the data at three temperatures (25, 30 and 35 °C), whereas the second value in parenthesis corresponds to the result with the data at 25 and 35 °C.

**Thermodynamic results**

$\Delta H^0$ = -15.6 (-16.1) kcal mol$^{-1}$ $\Delta C_p$ = 433 (444) cal mol$^{-1}$ K$^{-1}$

$K_d^0$ = 3.59 (3.61) µM

$\Delta S^0$ = -34 (-35.5 ) cal mol$^{-1}$ K$^{-1}$

**Kinetic results**

$k_{on}^0$ = 1912 (1848) M$^{-1}$ s$^{-1}$ $\Delta H_{on}^{\ddagger}$ = 16.5 (16.2) kcal mol$^{-1}$

$k_{off}^0$ = 0.00188 (0.00195) s$^{-1}$ $\Delta H_{off}^{\ddagger}$ = 34.4 (34.7) kcal mol$^{-1}$

### Results for the TPP riboswitch

The thermodynamic values marked with (ITC) correspond to the global values measured by ITC (*e.g.* $\Delta H^0$(ITC) = $\Delta H^0$(Binding) + $\Delta H^0$(Folding) or $K_d^0$ (ITC) = $K_d^0$ (Binding) /$K^0$(Folding)). The terms $\alpha$ and β refer to $\partial \Delta C_p$(ITC)/ $\partial T$ and $\partial \Delta C_p$(Folding)/ $\partial T$, respectively.

**Thermodynamic results**

$\Delta H^0$(ITC) = -21.8 kcal mol$^{-1}$ $\Delta C^0_p$ (ITC) = -1221 cal mol$^{-1}$ K$^{-1}$ $\alpha$ = -55 cal mol$^{-1}$ K$^{-2}$

$\Delta H^0$(Folding) = -32.1 kcal mol$^{-1}$ $\Delta C^0_p$(Folding) = -2245 cal mol$^{-1}$ K$^{-1}$ β = 38 cal mol$^{-1}$ K$^{-2}$

$K_d^0$ (ITC) = 0.024 µM $K_d^0$ (Binding) = 3.4 µM

$K^0$(Folding) = 140

$\Delta S^0$ = - 20 cal mol$^{-1}$ K$^{-1}$

**Kinetic results**

$k_{on}^0$ = 26200 M$^{-1}$ s$^{-1}$ $\Delta H_{on}^{\ddagger}$ (not defined)

$k_{off}^0$ = 0.09 s$^{-1}$ $\Delta H_{off}^{\ddagger} \approx$ -1.6 kcal mol$^{-1}$

$k_F^0$ = 1.1 s$^{-1}$ $\Delta H_F^{\ddagger} \approx$ 0.4 kcal mol$^{-1}$

$k_U^0$ = 0.008 s$^{-1}$ $\Delta H_U^{\ddagger} \approx$ 40 kcal mol$^{-1}$

## *References*

(1) Freire, E.; van Osdol, W. W.; Mayorga, O. L.; Sanchez-Ruiz, J. M. *Annu Rev Biophys Biophys Chem* **1990**, *19*, 159.
(2) Mayorga, O. L.; Freire, E. *Biophys Chem* **1987**, *27*, 87.
(3) Egawa T.; Tsuneshige A.; Suematsu M.; Yonetani T. *Anal Chem* **2007,** *79*, 2972.